Anomalous transport in biased ac-driven Josephson junctions: Negative conductances

M. Kostur,[1] L. Machura,[1] P. Talkner,[2] P. Hänggi,[2] and J. Łuczka[1]
[1]*Institute of Physics, University of Silesia, 40-007 Katowice, Poland*
[2]*Institute of Physics, University of Augsburg, D-86135 Augsburg, Germany*
(Received 30 November 2007; published 7 March 2008)

We investigate classical anomalous electrical transport in a driven, resistively, and capacitively shunted Josephson junction device. Intriguing transport phenomena are identified in chaotic regimes when the junction is subjected to both a time-periodic (ac) and a constant biasing (dc) current. The dependence of the voltage across the junction on the dc exhibits a rich diversity of anomalous transport characteristics. In particular, depending on the chosen parameter regime, we can identify the so termed absolute negative conductance around zero dc bias, the occurrence of negative differential conductance, and, after crossing a zero conductance, the emergence of a negative nonlinear conductance in the nonequilibrium response regime remote from zero dc bias.

DOI: 10.1103/PhysRevB.77.104509 PACS number(s): 74.25.Fy, 85.25.Cp, 73.50.Td, 05.45.−a

I. INTRODUCTION

The Josephson junction system constitutes a beautiful paradigm of a nonlinear system exhibiting most interesting classical and quantum phenomena.[1] This system, in addition, offers a rich spectrum of beneficial applications. For example, a prominent application of a Josephson junction setup relates to the definition of the voltage standard. Moreover, practical devices based on the characteristics of a Josephson junction are instrumental for high speed circuits: they can be designed to switch voltage within a few picoseconds. Their typical attribute of a low power dissipation proves them serviceable in high-density computer circuits, where the resistive heating limits the applicability of conventional switches. More recent applications refer to quantum computing devices where Josephson junction setups can store single units of information (qubits)[2] or, with appropriately engineered coupling among various units, they serve as an architecture for the processing of quantum information.[3] Yet, there still remain new phenomena to be uncovered for this system, which in turn carry the potential for new applications. Of special interest are novel transport phenomena in the presence of external ac and dc forcing. In this context, the phenomenon of absolute negative conductance (ANC) plays a particularly intriguing role. Here, ANC means that the system's response is *opposite* to a *small* external bias. In the present context, a small, say, positive dc generates a negative voltage across the junction. This constitutes no contradiction to thermodynamic laws because it occurs in the presence of simultaneously acting nonequilibrium perturbation, the ac drive. This phenomenon is known to emerge within a quantum mechanical setting in the presence of tunneling processes; remarkably, however, it has also been demonstrated on a classical level in stylized, spatially extended ratchetlike systems without reflection symmetry.[4–7]

The phenomenon of ANC has already been experimentally observed in *p*-modulation-doped GaAs quantum wells[8] and also in semiconductor superlattices, occurring therein as a genuine quantum phenomenon.[9] Interestingly enough, this very ANC phenomenon has been reported first in a recent work by us in Ref. 10 for an ac- and dc-driven Josephson junction. Notably, however, the study in Ref. 10 identifies this phenomenon within its *classical* operation regime for an inherent reflection-symmetric system. In extending our previous study in Ref. 10, we (i) provide further details, (ii) explore even wider regimes in parameter space, and (iii) identify additional unforeseen response regimes. In contrast to a related study,[11] where ANC is investigated in an underdamped, deterministic chaos regime, here, we emphasize the role of thermal noise and noise-induced nonlinear response phenomena. Moreover, we put forward a study of an accessible, optimal parameter regime toward the objective for an experimental verification of our findings. The underlying dynamics of this driven Josephson junction can conveniently be described by the model of a resistively and capacitively shunted junction in terms of the so-called Stewart–McCumber model.[1,12]

The layout of the present work is as follows. In Sec. II, we present the classical Stewart–McCumber model of the Josephson junction. Next, in Sec. III, we elucidate various regimes of anomalous transport behavior, such as ANC, negative differential conductance (NDC), and so termed negative-valued nonlinear conductance (NNC).

In Sec. IV, we work out the optimal regimes for the phenomenon of the negative conductance. In Sec. V, we elaborate on the experimental feasibility for an *in situ* confirmation of our diversified theoretical predictions. Section VI provides a summary and some conclusions.

II. STEWART–McCUMBER MODEL

This model describes the (semi)classical regime of the voltage-current characteristics of a Josephson junction. The model involves the Josephson supercurrent characterized by the critical current I_0, a normal (Ohmic) current characterized by the normal state resistance R, and a displacement current accompanied with the junction capacitance C. The ubiquitous thermal equilibrium noise consists of Johnson noise associated with the resistance R. The dynamics of the phase difference $\phi=\phi(t)$ across the junction is then described by the following nonlinear equation of motion, e.g., see in Ref. 12:

$$\left(\frac{\hbar}{2e}\right)^2 C\ddot{\phi} + \left(\frac{\hbar}{2e}\right)^2 \frac{1}{R}\dot{\phi} + \frac{\hbar}{2e} I_0 \sin(\phi) = \frac{\hbar}{2e} I_d + \frac{\hbar}{2e} I_a \cos(\Omega t) + \frac{\hbar}{2e}\sqrt{\frac{2k_B T}{R}}\xi(t). \quad (1)$$

Here, a dot denotes the differentiation with respect to time t, I_d and I_a are the amplitudes of the applied dc and ac, respectively, and Ω is the angular frequency of the ac driving. The parameter k_B denotes the Boltzmann constant and T is the temperature of the system. Thermal equilibrium fluctuations are modeled by δ-correlated Gaussian white noise $\xi(t)$ of zero mean and unit intensity, i.e., $\langle \xi(t)\xi(s)\rangle = \delta(t-s)$.

The limitations of the Stewart–McCumber model and its range of validity are discussed, e.g., in Secs. 2.5 and 2.6 of the comprehensive review paper by Kautz.[12] In particular, we thus work within the small junction area limit and in a regime where photon-assisted tunneling phenomena do not contribute. Throughout the following, we shall adopt the dimensionless form of Eq. (1) from Refs. 1 and 12, namely,

$$\frac{d^2\phi}{dt'^2} + \sigma\frac{d\phi}{dt'} + \sin(\phi) = i_0 + i_1 \cos(\Omega_1 t') + \sqrt{2\sigma D}\Gamma(t'), \quad (2)$$

where the dimensionless time $t' = t/\tau_0$ and the characteristic time $\tau_0 = 1/\omega_p$. The Josephson plasma frequency $\omega_p = (1/\hbar)\sqrt{8E_J E_C}$ is expressed by the Josephson coupling energy $E_J = (\hbar/2e)I_0$ and the charging energy $E_C = e^2/2C$. The "friction" coefficient $\sigma = \tau_0/RC$ is given by the ratio of two characteristic times: τ_0 and the relaxation time $\tau_r = RC$. This dimensionless friction parameter σ measures the strength of dissipation. The amplitude and the angular frequency of the ac are $i_1 = I_a/I_0$ and $\Omega_1 = \Omega\tau_0 = \Omega/\omega_p$, respectively. The rescaled dc reads $i_0 = I_d/I_0$, the rescaled zero-mean Gaussian white noise $\Gamma(t')$ possesses the autocorrelation function $\langle \Gamma(t')\Gamma(u)\rangle = \delta(t'-u)$, and the noise intensity $D = k_B T/E_J$ is given as the ratio of two energies, the thermal energy, and the Josephson coupling energy (corresponding to the barrier height). A different scaling procedure, being more familiar within the Brownian motor community, is detailed in the Appendix.

The most important characteristic for the above system is the current-voltage curve. To obtain it, we numerically integrated Eq. (2). For long time (to avoid initial conditions and transient effects), we calculated the stationary dimensionless voltage

$$v = \left\langle \frac{d\phi}{dt'} \right\rangle, \quad (3)$$

where the brackets denote an average over both all the realizations of the thermal noise and a temporal average over one cycle period of the external ac driving. The stationary physical voltage is then expressed as

$$V = \frac{\hbar\omega_p}{2e} v. \quad (4)$$

Strictly speaking, the zero temperature limit, $D=0$, should not be considered within the framework of the Stewart–McCumber model because at zero temperature, the quantum dynamics comes into play. However, in order to explain peculiar properties of the system at nonzero temperature and/or to seek optimal regimes, it is insightful nevertheless to consider the deterministic dynamics, i.e. the zero noise case, $D=0$. Then, the role of initial conditions is also relevant. This is particularly so if several attractors coexist. In such a case, an additional average over initial conditions must be performed. We have chosen initial phases ϕ_0 that are equally distributed over one period $[0, 2\pi]$ and (dimensionless) initial voltages v_0 equally distributed in the range $[-2, 2]$. Further details of how to treat the deterministic case are presented, e.g., in Ref. 13. In the case of several attractors, it means that the average is over attractors, whose weights are proportional to corresponding basins of attractions. However, it is worth stressing that the case $D=0$ generally is not equivalent to the limit $D \to 0$ performed in the nonzero temperature Fokker–Planck case (see the studies in Ref. 14).

Physical systems described by Eq. (2) are widespread and well known. An example is a Brownian particle moving in the spatially periodic potential $U(\phi) = U(\phi+L) = -\cos(\phi)$ of period $L = 2\pi$, driven by the time-periodic force and a constant force.[15] Then, the variable ϕ corresponds to the space coordinate of the Brownian particle and ac and dc play the role of driving forces on the particle. Other specific systems include rotating dipoles in external fields,[16,17] superionic conductors,[18] or charge density waves,[19] to name just a few.

III. ANOMALOUS TRANSPORT BEHAVIOR

The deterministic dynamics corresponding to Eq. (2) encompasses a three-dimensional phase space, namely, $\{\phi, d\phi/dt', \Omega_1 t'\}$ and contains four parameters, reading $\{\sigma, i_0, i_1, \Omega_1\}$. Therefore, its dynamics is able to exhibit an extremely rich behavior in phase space as a function of the chosen system parameters.[12,20] For example, its dynamics features harmonic, subharmonic, quasiperiodic, and also chaotic types of behavior; for further details, we refer the readers to the review in Ref. 12. At nonzero temperature, $D > 0$, thermal fluctuations lead to diffusive dynamics for which stochastic escape events among possibly coexisting attractors are possible.[21] Moreover, when thermal noise is acting, the system dynamics is constantly excited away from stable trajectories; it thus can explore the whole phase space. In some cases, the probability distribution can concentrate on regions in phase space which do not coincide with stable trajectories. The prominent example of such phenomena is a classical excitable stable point, which under influence of noise can produce a "limit-cycle-like" probability distribution.[22] This in turn can imply drastic consequences for the transport properties.

From the reflection symmetry $\phi \to -\phi$ of the potential $U(\phi) = -\cos(\phi)$ and the time reflection $t' \to -t'$ of ac driving, it follows that the average voltage is strictly *zero* if the dc is

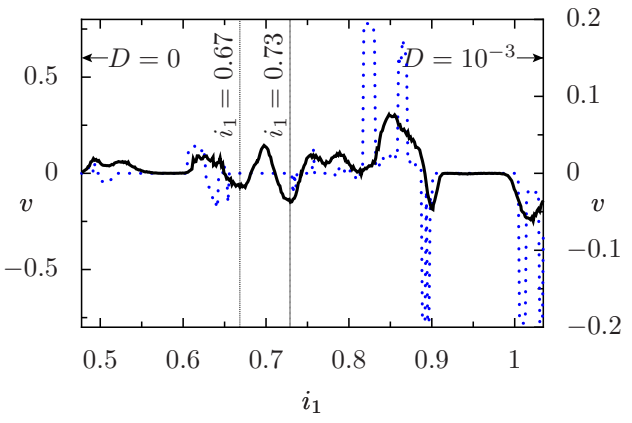

FIG. 1. (Color online) The diagram depicts the dependence of the voltage versus the variation of the driving amplitude i_1 of the ac for a positive dc set at $i_0=0.0159$. Remaining parameters are chosen as $\sigma=0.143$, $\Omega_1=0.78$, and temperatures $D=0$ [dotted line (blue), left scale] and $D=10^{-3}$ [solid line (black), right scale].

zero ($i_0=0$). If a nonvanishing dc is applied (i.e., $i_0\neq 0$), however, the above mentioned reflection symmetries are broken and a nonzero voltage typically emerges. Since the dynamics determined by Eq. (2) is nonlinear and the system is multidimensional, it should not come as a surprise that the current-voltage characteristic is typically nonlinear and often depicts a nonmonotonic function of the system parameters. Nevertheless, some most nonintuitive behaviors still remain to be unraveled in parameter space, which seemingly have escaped previous detailed investigations for this archetype system.[12]

The current-voltage curve $v=v(i_0)$ is a nonlinear function of the dimensionless dc strength i_0. Upon inspecting the symmetries in the equation of motion we find that this function is odd in the dc bias i_0, i.e., $v(-i_0)=-v(i_0)$. Typically, the voltage is an increasing function of dc. Such regimes correspond in parameter space to a normal, Ohmic-like transport behavior. More interesting are, however, those regimes of anomalous transport, exhibiting (i) a (absolute) negative conductance near zero dc bias, (ii) negative differential conductance, and (iii), after crossing zero conductance, a negative-valued conductance in a nonlinear regime displaced from zero dc bias $i_0=0$.

The numerical analysis of the system dynamics depicts that anomalous transport occurs in a parameter range where the driven system dynamics is strongly nonlinear. Although there is no obvious direct connection to chaotic properties of the system dynamics, we have found that regimes of anomalous transport typically necessitate also a chaotic dynamics. In particular, for the regime $\sigma=0.143$ and $\Omega_1=0.78$ presented in Fig. 1, the numerical study shows that the first bifurcation cascade at $D=0$ leading to chaos occurs near $i_1=0.477$ (cf. the dotted line in Fig. 1), while the regime of an anomalous transport behavior starts out near $i_1\simeq 0.637$. Not unexpectedly, no anomalous transport occurs in the regime of approximate linear dynamics.

A. Absolute negative conductance

In transport theory, the Green–Kubo linear response regime plays an important role. It allows one to obtain linear transport coefficients. For the system described by Eq. (2), there are regimes where for sufficiently small values of the dc bias i_0, linear response theory holds. This is characterized by the relation[23,24]

$$v = r_L i_0. \tag{5}$$

It defines the linear transport coefficient $r_L=r_L(\sigma,i_1,\Omega_1,D)$, which does not depend on i_0, and is called the static resistance or $g_L=1/r_L$ is the conductance in the linear response regime. Since the full response also exhibits a nonlinear behavior, it is necessary to recall that the resistance r_L is defined in the limit of a small dc, $r_L=\lim_{i_0\to 0}[v(i_0)/i_0]$. The case $r_L>0$ corresponds to the normal transport behavior or the Ohmic-like regime. The case $r_L<0$ amounts to the situation when the voltage assumes the opposite sign of the dc bias. It is termed here as the *absolute negative conductance* (in analogy to the absolute negative mobility of driven Brownian particles[4–7]). In Fig. 2, we exemplify this situation. Indeed, for dc values varying between $i_0\in(-0.04,0.04)$, the voltage assumes a sign opposite to i_0. The driving amplitude of the ac at $i_1=0.73$ corresponds to the second negative-valued minimum of the averaged voltage shown in Fig. 1 for a temperature $D=10^{-3}$. The first negative-valued minimum of v versus i_1 in Fig. 1 has been explored in greater detail in our previous work in Ref. 10. Let us emphasize here that, in distinct difference to this case with nonzero thermal noise $D\neq 0$, in the limit of vanishing noise (i.e., when $D=0$), the averaged voltage is, in fact, identically zero at the ac-driving strength $i_1=0.73$. This implies that this counterintuitive phenomenon of ANC is solely induced by *thermal equilibrium fluctuations*. For the record, there also exist linear response regimes where even in the deterministic case, the voltage can become negative for a positive dc (and vice versa).[10,11] From Fig. 1, one can observe that there exist several parameter windows depicting such a noise-induced ANC behavior: the conductance $g_L=g_L(\sigma,i_1,\Omega_1,D)$ exhibits sign changes multiple times upon increasing the ac-amplitude strength i_1. Between such ANC windows with $g_L<0$, normal transport regimes with $g_L>0$ occur. Moreover, we tested that the ANC windows remain stable upon a small variation of the remaining parameters.

B. Negative differential conductance

If the voltage v is not a monotonic function of the dc i_0, the *differential* conductance can assume negative values. The differential (or dynamic) resistance, defined by the relation[24]

$$r_D(i_0) = \frac{dv(i_0)}{di_0}, \tag{6}$$

may therefore assume negative values within some interval of dc-bias values i_0. In Fig. 2, we depict two examples of such behavior: the NDC $g_D(i_0)=1/r_D(i_0)$ is detected for the dc $i_0\in(0.0796,0.086)$ and $i_0\in(0.132,0.166)$, note the two inset panels in Fig. 2. To the best of our knowledge, this typical NDC voltage-current characteristic shown in Fig. 2 has not yet been experimentally reported for symmetrical systems, such as the system in Eq. (2). For asymmetric

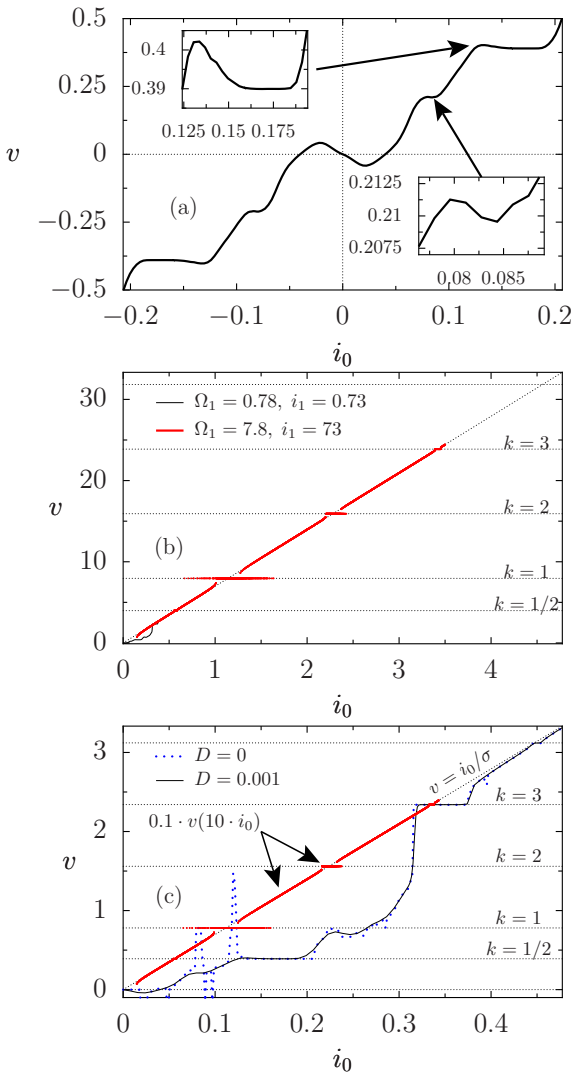

FIG. 2. (Color online) The functional dependence of voltage v on the dc current i_0 (i-v characteristic) is compared for two sets of parameters, which either display negative conductance or Shapiro steps. Panel (a), which corresponds to ac frequency $\Omega_1=0.78$, ac-driving strength $i_1=0.73$, friction $\sigma=0.143$, and noise strength $D=10^{-3}$, displays both absolute negative mobility in an interval containing $i_0=0$ and different regions with negative differential conductivity (cf. also the respective enlarged regions in the two insets). Panel (b) displays the i-v characteristic for the parameter values of panel (a) (thin solid line) and the i-v characteristic for $\Omega_1=7.8$, $i_1=73$, $\sigma=0.143$, and $D=0$ (thick solid line). Shapiro steps are clearly visible at $v=ki_0/\sigma$ for $k=1/2,1,2,3$ (dotted horizontal lines). Away from these steps, the i-v charateristic follows the Ohmic law $v=i_0/\sigma$ (dotted inclined line). Panel (c) presents the i-v characteristic for the small driving frequency ($\Omega_1=0.78$) for positive bias currents i_0 up to $i_0=0.48$ (solid line) and the i-v characteristic for the same set of junction parameters at zero noise ($D=0$) (dotted line with wide distance of dots) and compares them with a rescaled version $v_c:=0.1v(10i_0)$ of the i-v characteristic for the larger frequency such that the full range shown in panel (b) is displayed again. Whereas the linear overall behavior of the large frequency curve is interrupted only at a few Shapiro steps, the small frequency i-v characteristic is dominated by the nonlinearities also away from the locking regions at $v=\Omega_1/2$ and $v=3\Omega_1$.

ratchet systems, this effect was described in Ref. 25.

We note that both effects of absolute and differential negative conductance are found in the part of the Ω_1-σ plane, where $\Omega_1<1$ and $\Omega_1>\sigma$. In this region, Shapiro steps do not exist, i.e., there are no phase locked regions which interrupt an otherwise linear current current-voltage characteristic. For a detailed analysis of the different regions of the Ω_1-σ plane with respect to the occurrence of Shapiro steps, see the discussion in Sec. 5.1 of the review by Kautz.[12] In Fig. 2, current-voltage characteristics for two parameters sets $\Omega_1=0.78$, $\sigma=0.143$ and $\Omega_1=7.8$, $\sigma=0.143$ are displayed. The characteristics for the smaller frequency contain several bias current intervals with negative conductance and several locking regimes but no Shapiro steps. The second current-voltage characteristic does have pronounced Shapiro steps[26] but no regions with negative conductance.

C. Nonlinear response regime displaced from zero bias $i_0=0$: Negative-valued conductance

In the nonlinear response regime, the "nonlinear resistance" or the static resistance at a fixed bias current is defined by the relation[23,24]

$$r_N(i_0) = r_N(i_0;\sigma,i_1,\Omega_1,D) = \frac{v(i_0)}{i_0}. \tag{7}$$

It typically depends on i_0 in a nonlinear and nonmonotonic manner. The nonlinear conductance refers to its inverse, i.e., $g_N(i_0)=1/r_N(i_0)$. In the linear response regime, the voltage tends to zero when the dc tends to zero. In the nonlinear response regime, the voltage can tend to zero even if the dc assumes a nonzero, finite value. For example, two positive values of the dc $\{i_{01},i_{02}\}$ can emerge such that in between the voltage is negative. Then, the nonlinear conductance coefficient $g_N(i_0)$ is negative valued in this very interval (i_{01},i_{02}), which means that the voltage takes on the opposite sign of the dc for a nonzero valued dc-bias strength i_0. Indeed, this situation is presented in Fig. 3. The amplitude of the ac is set at $i_1=0.668$; it corresponds to the first negative-valued minimum of the averaged voltage depicted in Fig. 1. For small dc's, ANC exists (see inset of Fig. 3), while for larger dc's i_0, NNC results. NNC is a predominantly deterministic phenomenon which survives in the presence of small thermal noise. Indeed, we observe in Fig. 3 that for the case $D=0$, this effect is most pronounced and takes place in a wide parameter interval (i_{01},i_{02}). The long-time trajectories of the dynamical system [Eq. (2)] correspond to running states into the negative direction of ϕ, which are of period 2 and therefore the deterministic average voltage is large (cf. Fig. 3). When the temperature increases, the interval (i_{01},i_{02}) shrinks and the amplitude of the voltage decreases. Above some temperature ($D\approx 8\times 10^{-4}$ in Fig. 3), the NNC effect disappears and only ANC survives.

We end this section by a statement that the occurrence of anomalous transport may be governed by different mechanisms. In some regimes, it is solely induced by thermal equilibrium fluctuations, i.e., the effects are absent for vanishing thermal fluctuations, $D=0$. In other regimes, anomalous transport may also occur in the noiseless deterministic sys-

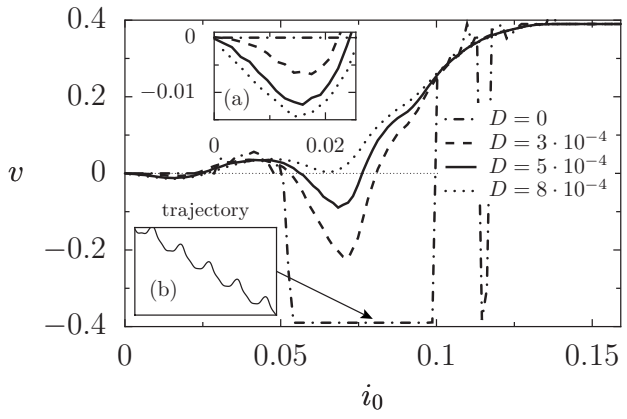

FIG. 3. Voltage vs dc: The reentrant effect of the negative response ($v<0$) is shown at a positive bias ($i_0>0$) for the following set of parameters: $i_1=0.668$, $\sigma=0.143$, $\Omega_1=0.78$, and four values of temperature D. For small i_0, the absolute negative conductance is observed for nonzero temperature and it is solely induced by thermal fluctuations [cf. panel (a)]. For larger i_0, negative nonlinear conductance results as a deterministic effect. The corresponding long-time trajectory $\phi(t')$ for $i_0=0.0796$ shown in panel (b) belongs to running states into the negative direction of ϕ resulting in the large average voltage. The value of the amplitude of ac driving corresponds to the first negative-valued minimum of the mean voltage with respect to the ac (cf. in Fig. 1).

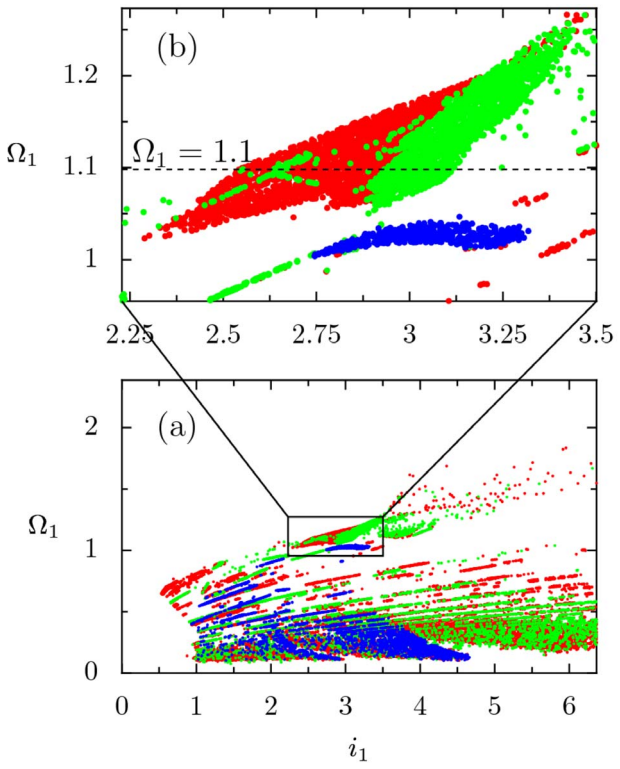

FIG. 4. (Color online) The transport properties of the driven system in the parameter space $\{i_1,\Omega_1\}$ at a representative friction value of $\sigma=0.191$, dc bias $i_0=0.0159$, and zero noise strength $D=0$. All points in the parameter space, where a negative conductance occurs, are marked by symbols with different gray scales. The coding corresponds to different regimes of values assumed by the ratio v/Ω_1: dark gray (red) denotes the interval $(-0.94,0)$, light gray (green) $(-1.26,-0.94)$, and black (blue) corresponds to values less than -1.26. Most of the dark gray points correspond to chaotic trajectories. It turns out that the black regimes are most susceptible to thermal fluctuations, which means that the negative-valued conductance rapidly fades away toward positive values with increasing thermal noise intensity. In panel (a), one clearly can distinguish a large compact region exhibiting negative-valued conductance, being enlarged with the upper panel (b). In regions different from this one, we find that negative-valued conductance occurs in narrow "bands" only. For an experimental realization of negative conductance, the most promising parameter regimes are those regions marked by light gray. This holds, in particular, for the zoomed light gray regimes depicted in panel (b).

tem and the effects increasingly fade out with increasing temperature.[10] Both situations are rooted in the complex deterministic structure of the nonlinear dynamics governed by a variety of stable and unstable orbits.

IV. OPTIMAL PARAMETER REGIMES FOR THE OCCURRENCE OF NEGATIVE CONDUCTANCE

In our recent work in Ref. 10 and in the previous section, we discussed some fixed parameters for $\{\sigma,\Omega_1\}$ for which the negative conductance (ANC or/and NNC) does emerge. Are these two values exceptional? To answer this question, we have searched the part of the three-dimensional parameter space that is specified by the ac-driving strength $\{i_1 \in (0,6.37)\}$, angular driving frequency $\{\Omega_1 \in (0,1.91)\}$, and friction strength $\{\sigma \in (0,0.796)\}$ in order to locate regions of negative conductances in the deterministic case, when $D=0$. We set the dc to a small value $i_0=0.0159$ and calculated the value of the current for many randomly chosen parameters i_1, Ω_1 and σ.[27] The inspection of the results revealed that there are values of friction σ for which regions of negative conductance are most prominent. One such value is $\sigma=0.191$ for which the negative conductance is most pronounced in a relatively large domain of parameter variation with relatively large values of the dimensionless voltage. Therefore, we performed a more accurate search for the section $\sigma=0.191$ and analyzed the two-dimensional parameter domain $\{i_1 \in (0,6.37),\Omega_1 \in (0,1.91)\}$. The results are depicted in Fig. 4. The points in Fig. 4 which are indicated by different gray scales correspond to values where $v(i_0=0.0159)<0$: the voltage assumes, thus, the opposite sign of the dc. Strictly speaking, a negative voltage at the finite bias $i_0=0.0159$ does not necessarily imply ANC. However, in most cases, under these conditions, ANC is observed in the presence of small thermal noise. We have also found that the noise-induced ANC typically occurs also for parameters which differ only slightly from those where $v(i_0=0.0159)<0$. Thus, this systematic analysis provides insight into the structure of the parameter space and proves useful for designing corresponding Josephson junction experiments. Finally, using extensively this technique, we are rather convinced that no remaining regimes of the negative conductance are likely to emerge in this system than those already depicted in Fig. 4. The gray scales in Fig. 4 represent various regimes of the

ratio v/Ω_1. One can distinguish two features in the parameter space: a stripelike structure for a broad range of parameters and one pronounced region, zoomed in panel (b). The stripelike structure suggests that in an experiment, one will observe with large probability negative conductance upon variation of a single parameter. In this context, the region shown in panel (b) is especially interesting because the negative conductance depicted there exhibits a relatively large robustness with respect to a variation of the system parameters.

In the deterministic case, we identify three classes of trajectories which generate negative conductance. This is marked by different gray scales in Fig. 4. Dark gray corresponds to chaotic trajectories. For this regime of parameters, the conductance is negative also for small nonzero temperatures. Light gray corresponds to periodic orbits. For this regime of parameters, the conductance is negative also for small nonzero temperatures. Black regions also correspond to periodic orbits; for this regime of parameters, the negative conductance, however, quickly diminishes as the temperature is raised.

From the experimental viewpoint, the most interesting regimes are those where the negative conductance is most robust within some finite temperature interval. In the case presented in Fig. 4, this corresponds to the dark and light gray regions. Therefore, we set, e.g., $\Omega_1=1.1$ [cf. panel (b) of Fig. 4], in order to observe the variation of the negative conductance when passing through the dark and light gray regions. Details are depicted in the bifurcation diagram (see Fig. 5). In the deterministic case, the voltage remains almost constant under small variations of the amplitude i_1 of the ac when the parameters belong to the light gray regions [note the voltage dependence on i_1 around $i_1=2.64$ and $i_1=3$ depicted in panel (a) of Fig. 5 for $D=0$]. On the other hand, the voltage changes irregularly when i_1 is changed smoothly within the red regions [note the voltage dependence on i_1 around $i_1=2.78$ depicted in panel (a) of Fig. 5 for $D=0$]. In Fig. 5, the averaged voltage is also shown for a small but nonvanishing temperature. When driving within the interval $a \in (2.55, 3.15)$, the voltage is negative for $D=10^{-3}$ and relatively stable with respect to a small variation of parameters. The region around $i_1=3$ lends itself as optimal for an experimental verification of our predicted anomalous transport features.

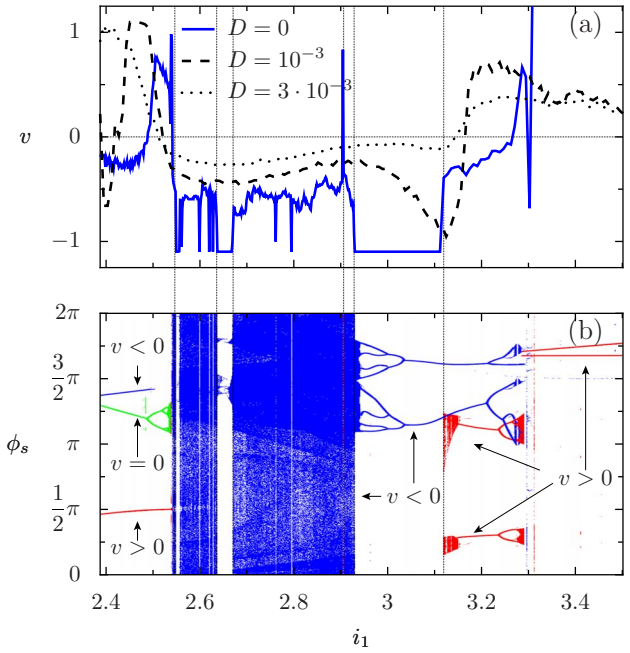

FIG. 5. (Color online) This figure elucidates the transport features and the dynamical properties for parameter values in $\{i_1, \Omega_1\}$ space within the section obtained by fixing the angular driving frequency at $\Omega_1=1.1$ [cf. the dotted line in panel (b) of Fig. 4]. The blue (solid) line in panel (a) depicts the dependence of the average voltage on the amplitude of the ac for zero noise $D=0$. The influence of thermal fluctuations on the average voltage is shown for two temperature values $D=10^{-3}$ (dashed line) and $D=3\times10^{-3}$ (dotted line). We do find that a negative-valued conductance indeed can survive at small nonzero temperatures. The transport properties of the system follow from the underlying complex dynamics. In panel (b), we show the bifurcation diagram: the Poincare section of the phase in the deterministic system. The attractors are color coded according to the sign of the assumed corresponding average voltage: blue yields a negative average voltage (also pointed by arrows with $v<0$), green gives zero (also pointed by arrows with $v=0$), and red amounts to a positive average voltage (also pointed by arrows with $v>0$).

V. EXPERIMENTALLY ACCESSIBLE REGIMES FOR ANOMALOUS TRANSPORT

The results presented above are given for dimensionless variables and dimensionless parameter values. In order to motivate experimentalists to test our predictions and findings, it is convenient to transform all quantities back to their original dimensional values and dimensional parameter strengths. There are three important parameters which characterize the function of a Josephson junction. These are the critical current I_0, the resistance R, and its capacitance C. Three further parameters characterize the external driving, namely, the strength of the dc I_d, the amplitude of the periodically varying ac I_a, and its angular frequency Ω. Finally, the temperature T must be chosen large enough such that the junction operates in the semiclassical regime. These physical quantities are related to the corresponding dimensionless quantities by the relations

$$V=\left(\frac{\hbar\omega_p}{2e}\right)v, \quad \Omega=\omega_p\Omega_1, \quad \frac{1}{RC}=\omega_p\sigma, \tag{8}$$

with the frequency scale ω_p given by the characteristic plasma frequency, which reads

$$\omega_p^2=\frac{2eI_0}{\hbar C}. \tag{9}$$

The driving strengths and the actual physical temperature read

$$I_a = I_0 i_1, \quad I_d = I_0 i_0, \quad T = \left(\frac{\hbar I_0}{2ek_B}\right) D, \tag{10}$$

being all scaled by the value of the critical current I_0.

First, one should fix the operational temperature T of the classical experimental regime. The last relation in Eq. (10) then yields the strength of critical current I_0. This in turn determines the amplitude strengths I_a and I_d. Fixing the frequency $\nu = \Omega/2\pi$ of the microwave source then determines via the chosen relevant value of the dimensionless parameter Ω_1 the strength of the plasma frequency ω_p. This in turn determines the magnitude of the capacitance C via the relation in Eq. (9), and the resistance R follows from the last relation in Eq. (8). Moreover, one should check whether the parameters such chosen obey the inequalities

$$\hbar\omega_p \ll E_J, \quad \hbar\omega_p \ll k_B T, \tag{11}$$

which, taken together, guarantee that the junction indeed operates in the (semi)classical regime, as presumed with Eq. (1). These inequalities imply that the level spacing of the plasma oscillation is small, both compared to the coupling energy E_J and the thermal energy $k_B T$.

To be explicit, we here evaluate some real experimental circumstances which can present "optimal" conditions to experimentally verify negative conductance. Upon inspection of our dimensionless analysis, the following parameter set is an example of the optimal regime: $i_1 = 3$, $\Omega_1 = 1.11$, $\sigma = 0.191$, and $D = 10^{-3}$. For a physical temperature of $T = 4$ K, the critical current is then $I_0 = 167.8$ μA, the amplitude strength becomes $I_a = 507$ μA, the ac-angular frequency emerges as $\Omega = 150$ GHz, and $I_d = 2{,}67$ μA with the capacitance being $C = 27.9$ pF and the resistance value at $R = 1.4$ Ω. Under these conditions, the absolute value of the voltage amounts to $V = 3.54$ μV.

The NDC regime, which is presented in Fig. 2, is observed for $i_1 = 0.73$, $\Omega_1 = 0.78$, $\sigma = 0.143$, and $D = 10^{-3}$, which for a temperature at $T = 4$ K implies a critical current $I_0 = 167.8$ μA, $I_a = 122$ μA, ac-angular frequency $\Omega = 150$ GHz, and I_d varying between $\in (13.36, 14.43)$ μA for $i_0 \in (0.0796, 0.086)$, with the capacitance set at $C = 13.83$ pF and the resistance set at $R = 2.63$ Ω. Under these conditions, the absolute value of the voltage approximately reads $V = 730$ μV.

VI. CONCLUSIONS

With this work, we took a closer look at the richness of anomalous transport behavior occurring in a biased and harmonically driven Josephson junction. As it turns out, the underlying chaotic dynamics together with the influence of thermal noise triggers a whole variety of unexpected transport features. Apart from regions displaying negative differential conductance behavior, we could identify different types of transport characteristics such as noise-induced absolute negative conductance near zero bias and negative-valued conductance in the strongly nonlinear response regime. Let us summarize these various transport phenomena occurring in an ac-driven Josephson junction as described by Eq. (1).

(1) The dependence of the voltage on the angular driving frequency Ω_1 of the ac drive depicts windows of deterministic and thermally induced ANC regimes: ANC appears and disappears as the frequency increases (for a preliminary account on this effect, see also Ref. 28).

(2) The dependence of voltage versus the amplitude i_1 of the ac drive depicts windows of thermal-noise-induced ANC regimes (cf. Fig. 1).

(3) The voltage behavior at fixed bias as a function of thermal temperatures D exhibits many familiar features known from the field of Brownian motors,[29] such as the occurrence of a voltage reversal versus D or a typical bell-shaped behavior versus noise strength D.[30]

(4) The voltage as a function of the bias current i_0 can exhibit each of the three anomalous transport features, namely, ANC, NNC, and NDC.

(5) Reentrant phenomena of negative conductance regimes occur as a function of the dc bias i_0. Starting out from zero, the voltage may decrease for increasing i_0, reaching a negative-valued local minimum value which changes over into a local positive-valued maximum upon increasing i_0. Upon further increasing i_0, the voltage starts to decrease again towards a local, negative-valued minimum, thus exhibiting NNC. Finally, it increases monotonically with increasing i_0, displaying an almost perfect Ohmic-like dependence.

Our identified transport features, as presented in Figs. 1 and 5, are also accessible to an experimental verification via appropriately designing the experimental working parameters for the Josephson system. Here, we identified such parameter sets Sec. V, while yet a different one has been indicated in our earlier presentation in Ref. 10. We are confident that our predictions will invigorate experimentalists to undertake the experimental efforts to check our various predictions.

ACKNOWLEDGMENTS

This work is supported by the DFG via Grant No. HA 1517/13-4, the DFG-SFB 486, the German Excellence Initiative via the *Nanosystems Initiative Munich* (NIM), Grant Nos. MNiSW N 202 131 32/3786, N202 203 534, and the DAAD-MNiSW program "Dissipative transport and ordering in complex systems."

APPENDIX

In our previous work,[10] we used a scaling popular among the "ratchet" community, where the "coordinate" variable $x = \phi/2\pi$ is rescaled to the unit interval. Then, the rescaled form of Eq. (1) reads

$$\ddot{x} + \gamma\dot{x} + 2\pi \sin(2\pi x) = f + a\cos(\omega s) + \sqrt{2\gamma D}\Gamma(s), \tag{A1}$$

where the dot denotes differentiation with respect to the dimensionless time $s = t/\tau_1$, where $\tau_1 = 2\pi/\omega_p$. The relations between the parameters in two scalings in Eqs. (2) and (A1) are as follows:

$$\gamma = 2\pi\sigma, \quad f = 2\pi i_0, \quad a = 2\pi i_1, \quad \omega = 2\pi\Omega_1. \tag{A2}$$

Now, the dimensionless velocity $v = \langle dx/ds \rangle$ and expressions for the voltage in Eq. (4) and the noise intensity D are identical for both scaling procedures.

[1] A. Barone and G. Paternò, *Physics and Application of the Josephson Effect* (Wiley, New York, 1982).
[2] Y. Makhlin, G. Schon, and A. Shnirman, Rev. Mod. Phys. **73**, 357 (2001).
[3] M. A. Sillanpaa, T. Lehtinen, A. Paila, Yu. Makhlin, L. Roschier, and P. J. Hakonen, Phys. Rev. Lett. **95**, 206806 (2005); T. Duty, G. Johansson, K. Bladh, D. Gunnarsson, C. Wilson, and P. Delsing, *ibid.* **95**, 206807 (2005).
[4] P. Reimann, R. Kawai, C. Van den Broeck, and P. Hänggi, Europhys. Lett. **45**, 545 (1999).
[5] R. Eichhorn, P. Reimann, and P. Hänggi, Phys. Rev. Lett. **88**, 190601 (2002).
[6] R. Eichhorn, P. Reimann, and P. Hänggi, Phys. Rev. E **66**, 066132 (2002).
[7] B. Cleuren and C. Van den Broeck, Phys. Rev. E **65**, 030101(R) (2002); A. Haljas, R. Mankin, A. Sauga, and E. Reiter, *ibid.* **70**, 041107 (2004).
[8] R. A. Höpfel, J. Shah, P. A. Wolff, and A. C. Gossard, Phys. Rev. Lett. **56**, 2736 (1986).
[9] B. J. Keay, S. Zeuner, S. J. Allen, Jr., K. D. Maranowski, A. C. Gossard, U. Bhattacharya, and M. J. W. Rodwell, Phys. Rev. Lett. **75**, 4102 (1995); L. Hartmann, M. Grifoni, and P. Hänggi, Europhys. Lett. **38**, 497 (1997); I. A. Goychuk, E. G. Petrov, and V. May, Phys. Lett. A **238**, 59 (1998); E. H. Cannon, F. V. Kusmartsev, K. N. Alekseev, and D. K. Campbell, Phys. Rev. Lett. **85**, 1302 (2000).
[10] L. Machura, M. Kostur, P. Talkner, J. Łuczka, and P. Hänggi, Phys. Rev. Lett. **98**, 040601 (2007).
[11] D. Speer, R. Eichhorn, and P. Reimann, Phys. Rev. E **76**, 051110 (2007).
[12] R. L. Kautz, Rep. Prog. Phys. **59**, 935 (1996).
[13] F. Family, H. A. Larrondo, D. G. Zarlenga, and C. M. Arizmendi, J. Phys.: Condens. Matter **17**, S3719 (2005).
[14] P. Jung and P. Hänggi, Phys. Rev. Lett. **65**, 3365 (1990); Ber. Bunsenges. Phys. Chem. **95**, 311 (1991).
[15] L. Machura, M. Kostur, F. Marchesoni, P. Talkner, P. Hänggi, and J. Łuczka, J. Phys.: Condens. Matter **17**, S3741 (2005); **18**, 4111 (2006); L. Machura, M. Kostur, P. Talkner, J. Łuczka, F. Marchesoni, and P. Hanggi, Phys. Rev. E **70**, 061105 (2004).
[16] D. Reguera, J. M. Rubi, and A. Pérez-Madrid, Phys. Rev. E **62**, 5313 (2000); D. Reguera, P. Reimann, P. Hänggi, and J. M. Rubi, Europhys. Lett. **57**, 644 (2002).
[17] W. T. Coffey, Yu. P. Kalmykov, and J. T. Waldron, *The Langevin Equation*, 2nd ed. (World Scientific, Singapore, 2004), Secs. 5 and 7–10.
[18] P. Fulde, L. Pietronero, W. R. Schneider, and S. Strässler, Phys. Rev. Lett. **35**, 1776 (1975); W. Dieterich, I. Peschel, and W. R. Schneider, Z. Phys. B **27**, 177 (1977); T. Geisel, Solid State Commun. **32**, 739 (1979).
[19] G. Grüner, A. Zawadowski, and P. M. Chaikin, Phys. Rev. Lett. **46**, 511 (1981).
[20] N. F. Pedersen, O. H. Soerensen, B. Dueholm, and J. Mygind, J. Low Temp. Phys. **38**, 1 (1980); M. Salerno, M. R. Samuelsen, G. Filatrella, S. Pagano, and R. D. Parmentier, Phys. Rev. B **41**, 6641 (1990); S. P. Kuznetsov and E. Neumann, Europhys. Lett. **61**, 29 (2003); E. Neumann and A. Pikovsky, Eur. Phys. J. B **34**, 293 (2003); V. E. Manucharyan, E. Boaknin, M. Metcalfe, R. Vijay, I. Siddiqi, and M. Devoret, Phys. Rev. B **76**, 014524 (2007).
[21] P. Hänggi, P. Talkner, and M. Borkovec, Rev. Mod. Phys. **62**, 251 (1990).
[22] M. Kostur, X. Sailer, and L. Schimansky-Geier, Fluct. Noise Lett. **2**, L155 (2003).
[23] H. Risken, *The Fokker-Planck Equation* (Springer, Berlin, 1989).
[24] E. Joergensen, V. P. Koshelets, R. Monaco, J. Mygind, M. R. Samuelsen, and M. Salerno, Phys. Rev. Lett. **49**, 1093 (1982); A. V. Ustinov and N. F. Pedersen, Phys. Rev. B **72**, 052502 (2005).
[25] M. Kostur, L. Machura, P. Hänggi, J. Łuczka, and P. Talkner, Physica A **371**, 20 (2006).
[26] K. O. Rasmussen, V. Zharnitsky, I. Mitkov, and N. Gronbech-Jensen, Phys. Rev. B **59**, 58 (1999); M. Moshe and R. G. Mints, *ibid.* **76**, 054518 (2007), and references therein.
[27] We have used the following percolationlike algorithm: starting from a point where the voltage is negative, we perturb the parameters by small random values and repeatedly calculate the voltage. When the local density of points with a negative voltage exceeds some prescribed value, a larger random perturbation is applied until we find a new region with a negative voltage. Then again, a search with small random perturbations was performed. Such an algorithm can be easily implemented on a PC cluster and yields a much better exploration of the parameter space than by a deterministic search on a regular mesh, especially in higher dimensions and for unknown ranges of parameters.
[28] L. Machura, M. Kostur, P. Talkner, P. Hänggi, and J. Łuczka, in *Noise and Fluctuations*, edited by M. Tacano, Y. Yamamoto, and M. Nakao, AIP Conf. Proc. No. 922 (AIP, Melville, NY, 2007), pp. 455–458.
[29] R. D. Astumian and P. Hänggi, Phys. Today **55** (11), 33 (2002); P. Reimann and P. Hänggi, Appl. Phys. A: Mater. Sci. Process. **75**, 169 (2002); P. Hänggi, F. Marchesoni, and F. Nori, Ann. Phys. **14**, 51 (2005).
[30] J. Łuczka, R. Bartussek, and P. Hänggi, Europhys. Lett. **31**, 431 (1995); J. Kula, M. Kostur, and J. Łuczka, Chem. Phys. **235**, 27 (1998); J. Kula, T. Czernik, and J. Łuczka, Phys. Rev. Lett. **80**, 1377 (1998); J. Łuczka, Physica A **274**, 200 (1999).